

RSC Advances



This is an *Accepted Manuscript*, which has been through the Royal Society of Chemistry peer review process and has been accepted for publication.

Accepted Manuscripts are published online shortly after acceptance, before technical editing, formatting and proof reading. Using this free service, authors can make their results available to the community, in citable form, before we publish the edited article. This *Accepted Manuscript* will be replaced by the edited, formatted and paginated article as soon as this is available.

You can find more information about *Accepted Manuscripts* in the [Information for Authors](#).

Please note that technical editing may introduce minor changes to the text and/or graphics, which may alter content. The journal's standard [Terms & Conditions](#) and the [Ethical guidelines](#) still apply. In no event shall the Royal Society of Chemistry be held responsible for any errors or omissions in this *Accepted Manuscript* or any consequences arising from the use of any information it contains.

ARTICLE

Separation of the Molecular Motion from Different Components or Phases using Projection Moving-Window 2D Correlation FTIR Spectroscopy for Multiphase and Multicomponent Polymers

Cite this: DOI: 10.1039/x0xx00000x

Received 00th January 2012,
Accepted 00th January 2012

DOI: 10.1039/x0xx00000x

www.rsc.org/

Tao Zhou,^{a,*} Ting Zhou,^a Aiming Zhang^a

This study developed a new analytical method called projection moving-window 2D correlation FTIR spectroscopy (Proj-MW2D) to separate the molecular motion of groups generated from different components or phases for multiphase and multicomponent polymers. The specific implementation steps for Proj-MW2D were enumerated after the theoretical derivation and algorithm research. Two types of two-component blends, poly(L-lactide)/poly(butylene succinate) and monodisperse polystyrene/monodisperse poly(ethylene-co-1-butene), were employed to validate the concept of separating the molecular motion of groups. Results showed that Proj-MW2D FTIR correlation technique successfully separated the molecular motion of the specific functional groups. Although MW2D and PCMW2D have the capacity to determine the multiple transitions of polymers, they cannot identify the origin of correlation intensity peaks without the help of other characterization methods. Proj-MW2D allows researchers to study the mechanism of the complex transition process for multiphase and multicomponent polymer systems. This method can be easily extended to three- or four-component polymers and to other spectra (e.g., Raman, X-ray, and UV).

1. Introduction

Polymers have a complex transition behavior. Since the discovery of polymers in organic materials chemistry, scientists have successfully developed numerous techniques to characterize polymer transition behavior.¹ The advancements in characterization methods have expanded our knowledge on polymer materials. Infrared (IR) spectroscopy is a classic method for polymers. It is a vibrational spectrum that reflects the dipole vibrations of specific bonds in polymers.^{2, 3} Therefore, IR spectroscopy provides molecular information at the functional group level.

Generalized 2D correlation vibrational spectroscopy, which was inspired from 2D NMR, was proposed by Noda in 1993.⁴ This technique uses Fourier transform and convolution to apply correlation analysis for in situ IR with an external perturbation.⁵ Peoples can employ it to study the interaction mechanism of functional groups in detail during polymer transitions. Given its practicality, generalized 2D correlation spectroscopy has rapidly become a new popular method of characterization.⁶⁻¹¹ However, 2D correlation spectroscopy cannot establish the relationship of correlation intensity peaks between spectral

variables (e.g., wavenumber, Raman shift) and external perturbation variables (e.g., temperature, pressure). Thomas and Richardson¹² proposed moving-window 2D correlation spectroscopy (MW2D) in 2000. The correlation intensity peaks of spectral variables directly associate with those of external perturbation variables in this technique; therefore, the transition points of polymers and the transition range can be precisely determined.¹³⁻¹⁹ Morita²⁰ introduced perturbation-correlation moving-window 2D correlation spectroscopy (PCMW2D) in 2006. Summary findings of scientists over many years found that the combination of MW2D or PCMW2D, and generalized 2D correlation spectroscopy was the best way.^{17, 18, 21-26} In general, MW2D or PCMW2D is employed to determine the transition point and the transition range of polymers; then, generalized 2D spectroscopy is performed to study the mechanism of functional groups at a specific transition.^{17, 18, 21-26} Compared with generalized 2D spectroscopy, 2D correlation spectroscopy with moving-window (MW2D or PCMW2D) has inherent advantages on studying the multiple transitions of polymers.

Generalized 2D correlation IR spectra are sometimes complex in practical applications. Specifically, the overlapping

of correlation peaks is serious or looks “crowded.” Explaining these spectra via Noda’s rules is difficult because of the interference of correlation intensity peaks.^{4,5} This phenomenon is obvious in multiphase and multicomponent polymer systems. In some block copolymers (SBS, SIS, and SEPS) and polymer blends, the correlation intensity peaks of minor components tend to be masked when main components dominate the transitions. Therefore, caution must be implemented when using generalized 2D correlation FTIR spectroscopy to study multiphase and multicomponent polymer systems. Considering this problem, Noda²⁷ proposed the projection technique for generalized 2D correlation spectroscopy in 2010. This method was extended from double 2D correlation analysis.²⁸ The projection technique was specifically developed for complex systems. This technique simplifies the “crowded” 2D correlation spectra by distinguishing the corresponding correlation intensity from different components. The concept of projection has aroused great interest among scientists.^{29, 30} However, generalized 2D correlation spectroscopy combined with projection still has some limitations on multiphase and multicomponent polymer systems because most polymers show multiple transitions under an external perturbation (e.g., temperature). Although MW2D or PCMW2D correlation spectroscopy has inherent capacity to determine the multiple transitions of polymers, it cannot identify the origin of correlation intensity peaks without the help of other characterization methods. To overcome these difficulties, this study developed a method called projection moving-window 2D correlation spectroscopy (Proj-MW2D) to separate the molecular motion of groups generated from different components in multicomponent polymers. The new approach not only has a capacity to precisely specify multiple transition points of polymers, but also can separate the molecular motion of groups. It will be particularly suitable to the study of the molecular movement mechanism of a specific transition for polymer systems.

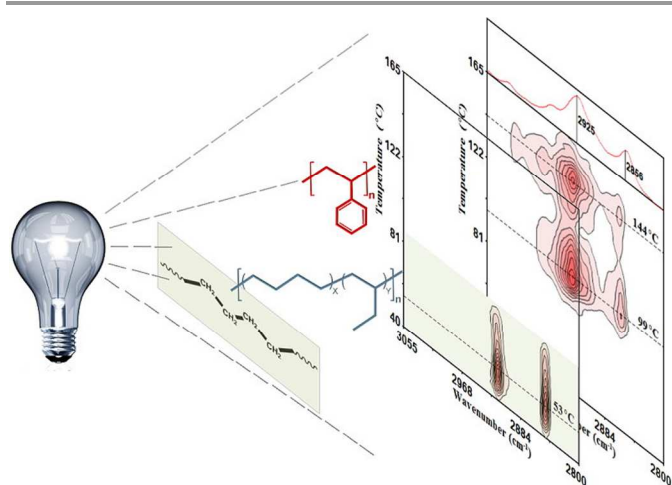


Figure 1. Schematic of the proposed concept of separating the molecular motion of groups from different components for multicomponent polymers.

In this paper, through theoretical derivation, algorithm research, and infrared spectroscopy experiments, the projection technique was successfully integrated into MW2D. **Figure 1** illustrates the proposed concept of separating the molecular motion of groups from different components. Proj-MW2D is a promising analytical method. This method possibly has potential outstanding and special applications in multiphase and multicomponent polymers.

2. Method

2.1. Spectral Data Matrix

The theoretical derivation of the method is outlined below.

Proj-MW2D needs to divide the entire spectral data matrix as a series of sub-matrices. Each sub-matrix is called as a window. A is supposed to be an $M \times N$ matrix of spectral data with M rows and N columns. ν and I represent the spectral variables (e.g., wavenumber) and external perturbation variables (e.g., temperature), respectively. Each row of A corresponds to the discrete data points of a spectrum.

$$A = \begin{pmatrix} y(\nu, I_1) \\ \vdots \\ y(\nu, I_j) \\ \vdots \\ y(\nu, I_M) \end{pmatrix} \quad (1)$$

The sub-matrix A_j is extracted from the main matrix A . At this point, the serial number of the perturbation variable I ranges from $j-m$ to $j+m$. Obviously, the sub-matrix A_j has $2m+1$ rows, whose column number is equal to the main matrix A . $2m+1$ is the window size.

The sub-matrix A_j can be expressed as

$$A_j = \begin{pmatrix} y(\nu, I_{j-m}) \\ \vdots \\ y(\nu, I_j) \\ \vdots \\ y(\nu, I_{j+m}) \end{pmatrix} \quad (2)$$

In general, the reference spectrum and the dynamic spectrum of the j th sub-matrix are calculated by the following formulas.

$$\bar{y}(\nu) = \frac{1}{2m+1} \sum_{J=j-m}^{j+m} y(\nu, I_J) \quad (3)$$

$$\tilde{y}(\nu, I_J) = y(\nu, I_J) - \bar{y}(\nu) \quad (4)$$

where J is a row number within a sub-matrix.

The mean-centered j th sub-matrix can be described as follows.

$$\tilde{A}_j = \frac{1}{\sqrt{2m}} \begin{pmatrix} \tilde{y}(v, I_{j-m}) \\ \vdots \\ \tilde{y}(v, I_j) \\ \vdots \\ \tilde{y}(v, I_{j+m}) \end{pmatrix} \quad (5)$$

2.2. Projection Matrix

A matrix Y has $2m+1$ rows and k columns, and the rows $(2m+1)$ of Y should be the same as those of \tilde{A}_j . The matrix Y reduces to a single vector y when Y has only one column.

The singular value decomposition (SVD) of matrix Y is defined as follows.

$$Y = U_Y S_Y V_Y^T + E_Y \quad (6)$$

SVD is a common method of extracting important features from a mathematical concept.³¹ It can be applied to an arbitrary matrix. SVD is attributed to the important field of data mining. Many applications can be related to SVD. These applications include PCA with the feature extraction, the data compression algorithm (represented by the image compression), and the latent semantic indexing for search engine.

U_Y is a matrix of $(2m+1) \times (2m+1)$. V_Y^T is a square matrix of $k \times k$. S_Y is a $(2m+1) \times k$ matrix, and its diagonal elements of $\sigma_1, \sigma_2, \dots, \sigma_k$ are the singular values of the matrix Y . E_Y is the residual matrix. Generally, it is small enough to be negligible. Here, we give an index r , which makes the value of $(\sigma_1 + \sigma_2 + \dots + \sigma_r) / (\sigma_1 + \sigma_2 + \dots + \sigma_r + \dots + \sigma_k)$ greater than or equal to 0.9 (90%), and the $1, \dots, (2m+1)$ rows and the $1, \dots, r$ columns of U_Y are used for the subsequent calculations.

Then, the projection matrix R_Y from Y can be calculated as:

$$R_Y = U_Y U_Y^T \quad (7)$$

R_Y is a $(2m+1) \times (2m+1)$ matrix. The used $(2m+1) \times r$ part of U_Y avoids R_Y transform to an identity matrix. The corresponding null-space projection matrix is defined as:

$$(I - R_Y) = I - U_Y U_Y^T \quad (8)$$

where I is the $(2m+1) \times (2m+1)$ identity matrix, Both R_Y and $I - R_Y$ are the symmetric matrix.

2.3. Generalized Projection Transformation

\tilde{A}_j matrix can be transformed into a new matrix of \tilde{A}_j^P with the projection according to the following formula:

$$\tilde{A}_j^P = R_Y \tilde{A}_j \quad (9)$$

The corresponding null-space projection matrix is:

$$\tilde{A}_j^N = \tilde{A}_j - \tilde{A}_j^P \quad (10)$$

In the j th sub-matrix, the projection synchronous and projection asynchronous 2D correlation spectra can be calculated as:

$$\Phi_j^P = (\tilde{A}_j^P)^T \cdot \tilde{A}_j^P \quad (11)$$

$$\Psi_j^P = (\tilde{A}_j^P)^T \cdot N \cdot \tilde{A}_j^P \quad (12)$$

The corresponding null-space projection synchronous and null-space projection asynchronous 2D correlation spectra are calculated as:

$$\Phi_j^N = (\tilde{A}_j^N)^T \cdot \tilde{A}_j^N \quad (13)$$

$$\Psi_j^N = (\tilde{A}_j^N)^T \cdot N \cdot \tilde{A}_j^N \quad (14)$$

where N is the *Hilbert-Noda* transformation matrix,⁵ which is a $(2m+1) \times (2m+1)$ matrix.

2.4. Positive Projection Transformation

According to Noda's proposal,²⁷ the loading matrix L of \tilde{A}_j^P is defined as:

$$L = \tilde{A}_j^T U_Y \quad (15)$$

Then, \tilde{A}_j^P can be expressed as:

$$\tilde{A}_j^P = U_Y L^T \quad (16)$$

In this study, we introduce a positive loading matrix L_+ , which comes from L by data processing. L_+ retains the elements of ≥ 0 in L , and the elements of < 0 are replaced by 0. After positive projection transformation, we obtain a new projection matrix \tilde{A}_j^{P+} . \tilde{A}_j^{P+} only reserves the columns in \tilde{A}_j^P that have the same change (or orientation) direction as in matrix Y .

$$\tilde{A}_j^{P+} = U_Y L_+^T \quad (17)$$

The corresponding null-space projection matrix is:

$$\tilde{A}_j^{N+} = \tilde{A}_j - \tilde{A}_j^{P+} \quad (18)$$

Then, the projection synchronous and projection asynchronous 2D correlation spectra in the j th sub-matrix are calculated as follows:

$$\Phi_j^{P+} = (\tilde{A}_j^{P+})^T \cdot \tilde{A}_j^{P+} \quad (19)$$

$$\Psi_j^{P+} = (\tilde{A}_j^{P+})^T \cdot N \cdot \tilde{A}_j^{P+} \quad (20)$$

The corresponding null-space projection synchronous and null-space projection asynchronous 2D correlation spectra are calculated as follows:

$$\Phi_j^{N+} = (\tilde{A}_j^{N+})^T \cdot \tilde{A}_j^{N+} \quad (21)$$

$$\Psi_j^{N+} = (\tilde{A}_j^{N+})^T \cdot N \cdot \tilde{A}_j^{N+} \quad (22)$$

2.5. Moving-window

A series of sub-matrices are obtained by sliding the window position from $j=I+m$ to $j=M-m$. The calculations are repeatedly performed using the above equations for each sub-matrix (window). Then, an overlay operation that is identical to the conventional MW2D algorithm is employed to gain a Proj-MW2D correlation spectrum^{13, 17} and a null-space Proj-MW2D correlation spectrum. For convenient explanation and calculations, our study focuses on Proj-MW2D and null-space Proj-MW2D based on auto-correlation.

2.6. Multiple Projection for Three to Four Components (or Phases)

The algorithm mentioned above is only applicable to polymers with two components (or phases). The multiple projection operation should be introduced to investigate three- to four-component (phases) polymers.

\tilde{A}_j^N or \tilde{A}_j^{N+} is specified as a new spectral data matrix. We select matrix Y_l as another projection to repeat equations (6) to (10) or (15) to (18). Then, the spectral data matrix \tilde{A}_j^{Pl} or \tilde{A}_j^{Pl+} with the second projection and the spectral data matrix \tilde{A}_j^{Nl} or \tilde{A}_j^{Nl+} with null-space second projection are obtained.

$$\tilde{A}_j^{Pl} = R_{Y_l} \tilde{A}_j^N \quad (23)$$

$$\tilde{A}_j^{Nl} = \tilde{A}_j^N - \tilde{A}_j^{Pl} \quad (24)$$

$$\tilde{A}_j^{Pl+} = U_{Y_l} L_{Y_l}^T \quad (25)$$

$$\tilde{A}_j^{Nl+} = \tilde{A}_j^{N+} - \tilde{A}_j^{Pl+} \quad (26)$$

This algorithm allows Proj-MW2D to analyze polymer systems with three components (or phases). Similarly, using \tilde{A}_j^{Pl} or \tilde{A}_j^{Pl+} as a new spectral data matrix for the third projection, we can use Proj-MW2D to analyze polymer systems with four components (or phases).

2.7. Selection of the Projection Matrix Y

The projection matrix Y influences the final results. The matrix Y can be selected from the j th sub-matrix \tilde{A}_j , which has the mean-centered processing. Generally, the matrix Y contains a few columns of \tilde{A}_j . In the actual spectrum (e.g., IR), these columns contain some characteristic bands. It degenerates into a vector when Y has only one column of \tilde{A}_j , which corresponds to a characteristic spectral peak. Selecting the projection matrix Y from the spectral data matrix \tilde{A}_j can satisfy most of our needs. The projection matrix Y can also be chosen from other sources, such as from another experiment of IR or Raman spectra.

External perturbations (such as temperature or concentration) can be also selected as the projection matrix Y . In some cases, specific mathematical functions can be used as a projection matrix for model-based analyses. In Proj-MW2D correlation spectroscopy, the construction method of the projection matrix Y is similar to Noda's proposal.

2.8. Implementation Steps for Polymers

Polymer blends with two components (or phases), such as A+B, are used as an example to show the implementation steps of Proj-MW2D in separating the molecular motion of groups. The basic steps are outlined below:

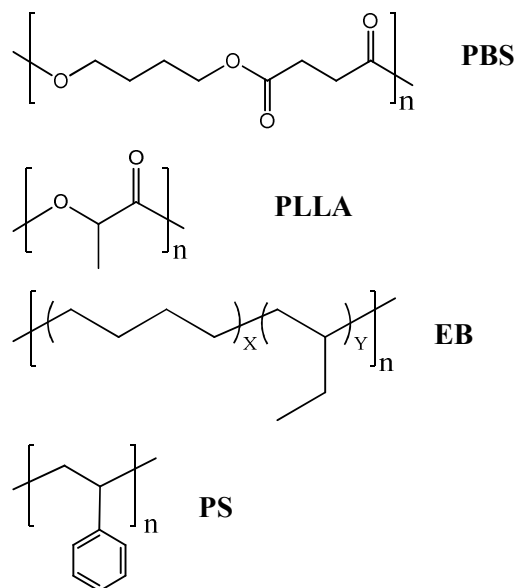
- 1) In situ spectral data of polymer blend samples are collected in the presence of an external perturbation (temperature, concentration, etc.). Collecting the maximum number of spectra ensured by the signal-noise ratio and allowed by the spectrometer collection rate is recommended to accurately describe the physical or chemical processes of the samples.
- 2) The projection matrix Y is constructed. In general, Y is selected from the interest characteristic bands in the in situ spectral data. For multiphase and multicomponent polymers, Y is often chosen from the most characteristic bands that can represent a phase or a component. This characteristic bands can distinguish the interest component from the other components (or phases). For two-component polymer blends, we choose certain characteristic bands of component A (denoted as a) to construct the projection matrix.
- 3) Proj-MW2D correlation spectra are calculated using the positive projection transformation algorithm. The algorithm can be compiled into program using C and C++ computer language or using Matlab directly.
- 4) Proj-MW2D correlation spectrum and null-space Proj-MW2D correlation spectrum are obtained. For two-component polymer blends, the response of correlation intensities from component A appear in Proj-MW2D correlation spectra, and the response of correlation intensity from component B presents in null-space Proj-MW2D correlation spectra. The reason for this result is that the response with the same variation feature as the characteristic bands (a) of component A is retained by the positive projection algorithm.
- 5) The transition range of components A and B is determined according to the response of the correlation intensity. The individual physical and chemical transitions of A or B and collaborative transitions of A+B involved can be identified. Then, the mechanism and bands' assignment can be further analyzed.

3. Experimental Section

In this study, two types of two-component polymer blends were prepared using different blending methods. The molecular motion of groups generated from different components was separated using Proj-MW2D correlation analysis.

3.1. Materials

Poly(L-lactide) (4032D) was provided by NatureWorks LLC, USA. Poly(butylene succinate) (Bionolle 1001MD) was provided by Showa Highpolymer Co., Ltd., Japan. Monodisperse polystyrene (PS) and monodisperse poly(ethylene-co-1-butene) (EB, also known as fully hydrogenated polybutadiene) synthesized via anionic polymerization were supplied by Baling Petrochemical Industry Co., Ltd. (Sinopec). Cyclohexane with 99.5% (AR) purity was produced by Chemical Reagent Union Co., Ltd. The weight average molecular weight of monodisperse PS was 10,000 g/mol, and its monodisperse coefficient was 1.04 (GPC). The weight average molecular weight of monodisperse EB was 120,000 g/mol, and its monodisperse coefficient was 1.05 (GPC). The molar content of 1-butene in EB was 29% (NMR). Poly(butylene succinate) (PBS), poly(L-lactide) (PLLA), monodisperse polystyrene (PS), and monodisperse poly(ethylene-co-1-butene) (EB) were directly used without further purification. The molecular structures of these materials are shown in **Scheme 1**.



Scheme 1. Molecular structures of PBS, PLLA, EB, and PS.

3.2. Preparation

3.2.1. PLLA/PBS blend

PBS and PLLA pellets were vacuum-dried at 70 °C for 24 h. A PLLA/PBS blend was prepared by a twin-screw extruder through melt blending. The weight ratio of PLLA and PBS was 50:50. The temperature of melt blending ranged from 175 °C to 185 °C, and the screw speed was 180 rpm.

3.2.2. PS/EB Blend

A PS/EB blend was prepared by solution blending. Monodisperse PS (0.714 g) and monodisperse EB (4.286 g) were simultaneously dissolved in 250 ml of cyclohexane. After becoming transparent, the solution was stored under an air-tight seal for 4 d before use.

3.3. Temperature-dependent FTIR Spectroscopy

A Nicolet iS10 FTIR spectrometer equipped with a deuterated triglycine sulfate detector was used. The FTIR spectral resolution was 4 cm⁻¹, and 20 scans were co-added for each FTIR spectrum.

3.3.1. PLLA/PBS

A pellet (0.5 g) of the PLLA/PBS blend was placed between two polyethylene terephthalate (PET) sheets. The film was directly prepared by heat-pressing the PLLA/PBS blend sandwiched between two PET sheets at 185 °C in a hot press and then allowing the blend to naturally cool at room temperature. The heat-pressing time was 2 min, and the pressure was 20.0 MPa. Then, the film was cut into a circular shape (Φ1.3 cm). The film was sandwiched between two KBr windows to prevent high-temperature flow and then placed into a homemade in situ pool (programmable heating device). The sample film was heated from 20 °C to 120 °C at 5 °C/min and then was stored at 120 °C for 3 min. The molten sample was cooled from 120 °C to 50 °C at 5 °C/min. Meanwhile, the FTIR spectra were collected from 120 °C to 50 °C. Thirty-three FTIR spectra were collected upon cooling. The sample was protected by dried high-purity nitrogen gas (300 ml/min) during the measurement.

3.3.2. PS/EB

A film of the PS/EB blend was spread on one side of a KBr disk by solvent casting from the solution prepared in **Section 3.2.2**. The film was dried in a vacuum oven at 90 °C for 120 min at -0.08 MPa. The sample film was sandwiched between two KBr disks and then placed into a homemade in situ pool. The sample was heated from 30 °C to 175 °C at 5 °C/min. The FTIR spectra were collected from 30 °C to 175 °C at approximately 2.1 °C increments. The number of the spectra collected was 68. The sample was also protected by dried high-purity nitrogen gas.

3.4. Proj-MW2D Correlation Analysis

Proj-MW2D correlation FTIR spectra were processed and calculated using 2DCS 6.1 software, developed by one of the authors using Visual C++. Before the analysis, the IR spectra were treated using a linear baseline correction. The window size was chosen as $2m+1=11$ to produce high-quality Proj-MW2D FTIR spectra and null-space Proj-MW2D FTIR spectra. The 1% correlation intensity of the Proj-MW2D and null-space Proj-MW2D correlation spectra was regarded as noise and was cut off. In the 2D spectra, red and blue areas represent positive and negative correlation intensities, respectively.

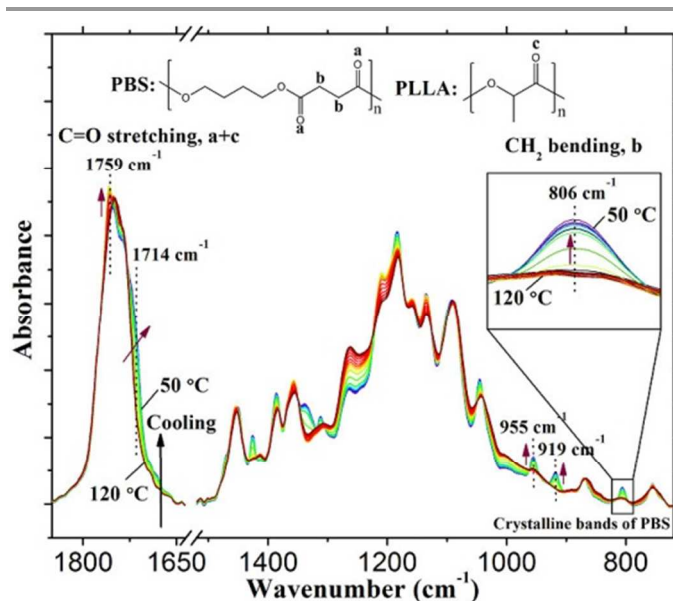


Figure 2. Temperature-dependent FTIR spectra of PLLA/PBS in the 1850 cm^{-1} to 720 cm^{-1} region upon cooling ($120\text{ }^{\circ}\text{C}$ to $50\text{ }^{\circ}\text{C}$). The region from 1635 cm^{-1} to 1520 cm^{-1} is truncated. The bands within 1850 cm^{-1} to 1635 cm^{-1} , which is the overlapping of PBS and PLLA, are assigned to the C=O stretching vibration. The bands at 806 cm^{-1} is the CH_2 in-plane bending in the $\text{OC}(\text{CH}_2)_2\text{CO}$ of the PBS component, and it is chosen as the projection vector. The FTIR spectra at 806 cm^{-1} are enlarged for clarity. For clear illustration, not all the collected FTIR spectra are shown.

4. Results and Discussion

4.1. Separation of the Molecular Motion of C=O Groups from the Crystalline Phase of the PBS Component during PLLA/PBS Crystallization upon Cooling

4.1.1. Temperature-dependent FTIR of PLLA/PBS Crystallization

PBS and PLLA are completely biodegradable plastics.³²⁻³⁵ The temperature-dependent FTIR spectra of PLLA/PBS in the 1850 cm^{-1} to 720 cm^{-1} region upon cooling are shown in **Figure 2**. The region within 1635 cm^{-1} to 1520 cm^{-1} is an entirely horizontal baseline; thus, the spectra in this range are truncated. For the sake of clarity, **Figure 2** does not show all the collected spectra. The bands' assignments are listed in **Table 1**. This study focuses on the bands within the 1850 cm^{-1} to 1635 cm^{-1} region. These bands, which are the overlapping of PBS and PLLA, are assigned to the C=O stretching vibration of PBS and PLLA.³⁶⁻⁴¹ Some minor changes are observed within 1850 cm^{-1} to 1635 cm^{-1} when the temperature decreases from $120\text{ }^{\circ}\text{C}$ to $50\text{ }^{\circ}\text{C}$. The peak intensity at 1759 cm^{-1} gradually increases, whereas the bands at 1714 cm^{-1} slightly move to the lower wavenumber. These results show that temperature-dependent FTIR cannot separate the molecular motion from the C=O groups in the PBS crystalline phase. Our target is to use Proj-MW2D to separate the C=O motion generated from the PBS crystalline phase during PLLA/PBS crystallization.

Table 1. Band Assignments of PLLA, PBS, PS, and EB.

Wavenumber (cm^{-1})	Assignment	
	PLLA	PBS
1759	C=O stretching vibration	--
1714	--	C=O stretching vibration
955 (960–930)	CH_3 rocking+C–C stretching	C–O symmetric stretching
919 (924–920)	10^3 helical chain skeletal deformation	CH_2 skeletal deformation
806	--	CH_2 in-plane bending in $\text{OC}(\text{CH}_2)_2\text{CO}$
	PS	EB
2925	CH_2 antisymmetric stretching vibration of the main chain	CH_2 antisymmetric stretching vibration
2856	CH_2 symmetric stretching vibration of the main chain	CH_2 symmetric stretching vibration
1462	--	CH_2 bending vibration
1453	CH_2 bending vibration of the main chain	--
757	=CH out-of-plane bending vibration of benzene rings	--
720	--	CH_2 rocking of the ethylene units
698	=CH out-of-plane bending vibration of benzene rings	--

4.1.2. Selection of Projection Vector

Determining the projection matrix (or vector) is crucial. Because we want to separate the molecular motion of C=O groups from PBS crystalline phase, the projection matrix (or vector) should be the characteristic bands of PBS and the bands can accurately describe the functional group movements of the PBS crystalline phase during crystallization. In addition, the bands should not overlap with any bands of the PLLA component. In **Figure 2**, also refer to the literature,^{38, 42} we find three characteristic bands of PBS at 955 , 919 , and 806 cm^{-1} . The bands at 955 cm^{-1} is assigned to the C–O symmetric stretching of PBS.⁴² The bands at 919 cm^{-1} is attributed to the CH_2 skeletal deformation of PBS,^{38, 42} and that at 806 cm^{-1} is attributed to the CH_2 in-plane bending in $\text{OC}(\text{CH}_2)_2\text{CO}$.⁴² These three bands can be judged as the crystallization bands of PBS because their intensities gradually increase as the temperature decreases from $120\text{ }^{\circ}\text{C}$ to $50\text{ }^{\circ}\text{C}$. The crystallization behavior of PBS in PLLA/PBS is clearly described by 955 , 919 , and 806 cm^{-1} upon cooling. However, according to the literature,^{43, 44} the bands in the 960 cm^{-1} to 930 cm^{-1} and 924 cm^{-1} to 920 cm^{-1} regions are also assigned to the CH_3 rocking+C–C stretching and 10^3 helical chain skeletal deformation of the PLLA component, respectively. Therefore, in **Figure 2**, only 806 cm^{-1} is fully attributed to PBS. The bands at 806 cm^{-1} does not overlap with any bands of PLLA, and it accurately describes the crystallization behavior of PBS. The molecular structure of PBS also shows that the corresponding CH_2 groups of 806 cm^{-1} directly connect to the C=O groups, thereby reflecting the real C=O movements of PBS. In this study, the bands at 806 cm^{-1} is certainly chosen as the projection. To simplify the calculations, we only select the spectral intensity at 806 cm^{-1} as the

projection. Thus, the projection vector (not a matrix) is the spectral intensity at 806 cm^{-1} .

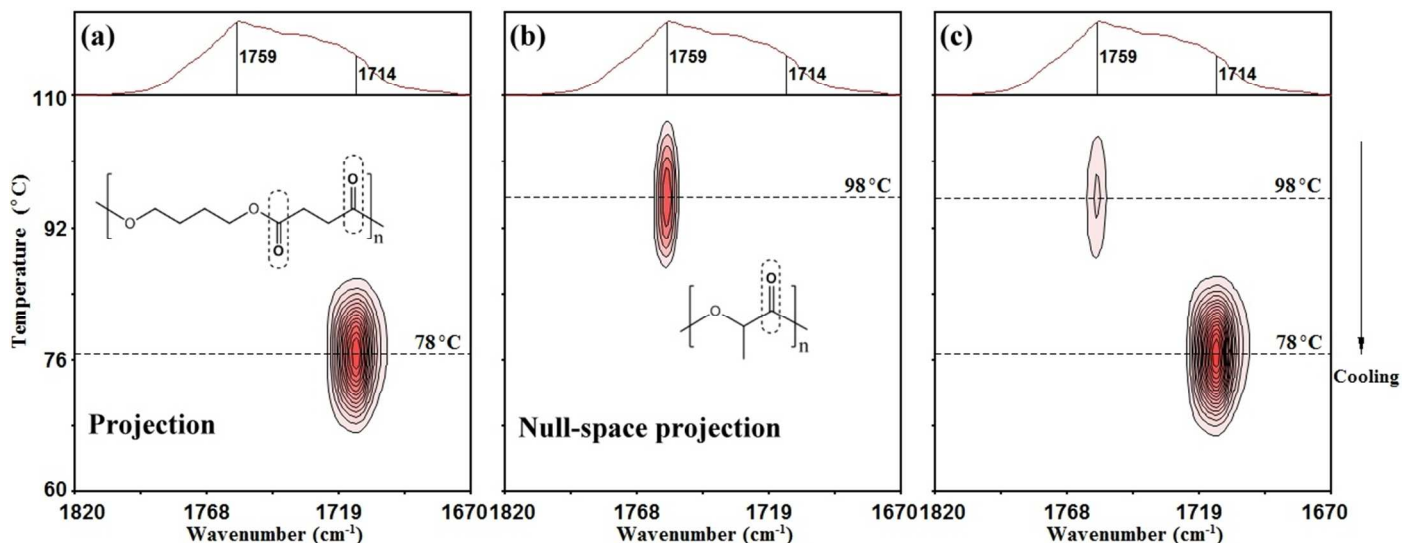


Figure 3. Key: (a) Proj-MW2D correlation FTIR spectrum of PLLA/PBS ($110\text{ }^{\circ}\text{C}$ to $60\text{ }^{\circ}\text{C}$); (b) null-space Proj-MW2D correlation FTIR spectrum of PLLA/PBS ($110\text{ }^{\circ}\text{C}$ to $60\text{ }^{\circ}\text{C}$); (c) conventional MW2D correlation FTIR spectrum ($110\text{ }^{\circ}\text{C}$ to $60\text{ }^{\circ}\text{C}$). The positive projection transformation algorithm is used for the calculations. The molecular motion of the C=O groups involved in the crystallization of the PBS component is retained in the Proj-MW2D correlation spectrum, and the response temperature is approximately $78\text{ }^{\circ}\text{C}$. The C=O motion of the PLLA component ($98\text{ }^{\circ}\text{C}$) appears in the null-space Proj-MW2D correlation spectrum.

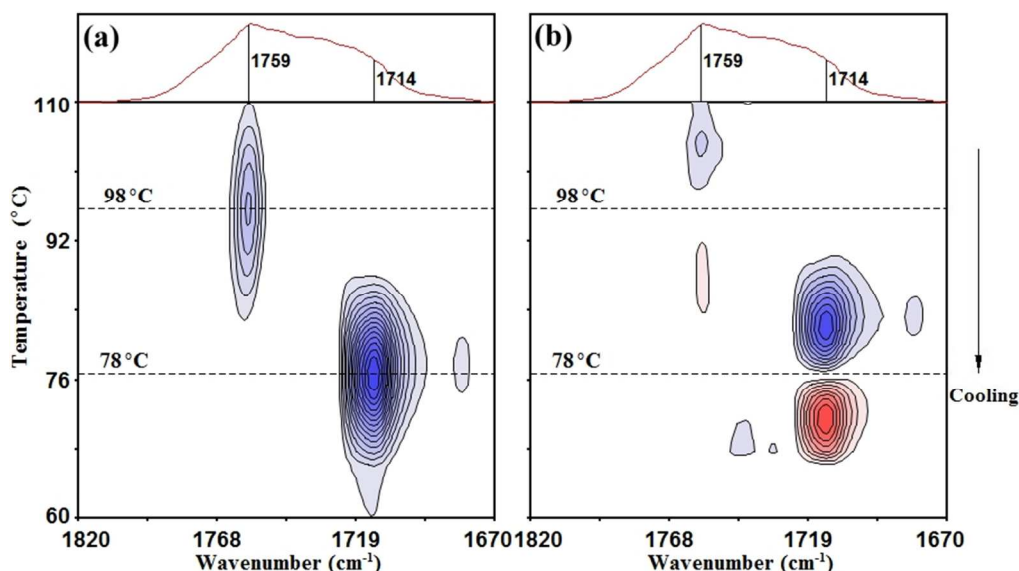


Figure 4. Key: (a) synchronous PCMW2D correlation FTIR spectrum of PLLA/PBS ($110\text{ }^{\circ}\text{C}$ to $60\text{ }^{\circ}\text{C}$) upon cooling; (b) asynchronous PCMW2D correlation FTIR spectrum of PLLA/PBS ($110\text{ }^{\circ}\text{C}$ to $60\text{ }^{\circ}\text{C}$) upon cooling.

4.1.3. Proj-MW2D Analysis of the Molecular Motion of the C=O Groups

Figure 3 is the Proj-MW2D correlation FTIR spectra of PLLA/PBS upon cooling, and the spectral intensity at 806 cm^{-1} is the projection vector. **Figures 3(a)** and **3(b)** show the Proj-MW2D correlation spectrum and null-space Proj-MW2D correlation spectrum, respectively.

The molecular motion of the C=O groups with the same motion feature as the projection vector at 806 cm^{-1} is retained in the Proj-MW2D correlation spectrum [**Figure 3(a)**]. Results

show that the correlation intensity appears at approximately 1714 cm^{-1} , which represents the C=O motion involved in PBS crystallization. The response temperature is approximately $78\text{ }^{\circ}\text{C}$. This temperature is the crystallization temperature of PBS in PLLA/PBS. In the null-space Proj-MW2D correlation spectrum [**Figure 3(b)**], the C=O motion that is completely orthogonal (not identical) with the projection vector at 806 cm^{-1} is observed. **Figure 3(b)** represents the molecular motion of the C=O groups of PLLA because 806 cm^{-1} is attributed to the PBS component. In **Figure 3(b)**, the corresponding correlation intensity is observed at around 1759 cm^{-1} , and the

response temperature is 98 °C. Therefore, the crystallization temperature of PLLA is 98 °C under the experimental conditions described in the present study.

Aside from separating the molecular motion of functional groups from the different components, Proj-MW2D correlation analysis can also be used to assign the overlapping bands. In **Figures 3(a)** and **3(b)**, it can be easily distinguished that the crystalline bands of PBS and PLLA are 1714 and 1759 cm^{-1} , respectively. This result is similar to previous reports.^{37, 39, 41-44} However, these reports used conventional FTIR, and their experimental methods were more complex than the ones used in the present study. In addition, these reports used the pure substance to confirm the assignment of PLLA, whereas we directly specified the assignment at 1714 and 1759 cm^{-1} from the PLLA/PBS blend. Therefore, Proj-MW2D correlation analysis also provides a simple way to determine the spectral assignments for multiphase and multicomponent polymers.

Figure 3(c) shows the conventional MW2D correlation FTIR spectrum of the PLLA/PBS blend for comparison. The conventional MW2D correlation FTIR spectrum is the combination of the Proj-MW2D [**Figure 3(a)**] and null-space Proj-MW2D correlation FTIR spectra [**Figure 3(b)**]. However, in-depth analysis shows that the conventional MW2D method can only determine two transition temperatures of PLLA/PBS upon cooling. In addition, it cannot specify the origin of the molecular motion of the C=O groups in the 1850 cm^{-1} to 1635 cm^{-1} region. The PCMW2D correlation FTIR spectra of the PLLA/PBS blend upon cooling are illustrated in **Figure 4**, including synchronous [**Figure 4(a)**] and asynchronous spectra [**Figure 4(b)**]. Similarly, PCMW2D can determine two transitions of PLLA/PBS at 98 °C and 78 °C, respectively. However, similar to conventional MW2D, PCMW2D also cannot specify the origin of the C=O motion at 1759 and 1714 cm^{-1} . In **Figure 4(a)**, the negative correlation peaks of blue areas represent the increase in the spectral intensities at 1759 and 1714 cm^{-1} in the cooling direction.

4.2. Extraction of the Molecular Motion of CH₂ Groups from Ethylene Units in the EB Component during Microcrystalline Melting in PS/EB

4.2.1. Temperature-dependent FTIR of PS/EB

The monodisperse PS and EB are thermodynamically incompatible. The molar content of the ethylene unit in EB was 71% (measured by NMR); thus, the ethylene units can form some microcrystals.^{17, 45-47} The monodisperse PS used in this study is atactic PS. **Figure 5** shows the temperature-dependent FTIR spectra of PS/EB in the 3055 cm^{-1} to 630 cm^{-1} region upon heating (30 °C to 175 °C). The bands' assignments are listed in **Table 1**. The bands within the 3055 cm^{-1} to 2800 cm^{-1} region (**Figure 5**) show serious overlapping, particularly at 2925 and 2856 cm^{-1} . The bands at 2925 and 2856 cm^{-1} correspond to the antisymmetric and symmetric stretching vibrations of CH₂, respectively.⁴⁸ However, not only are these

bands assigned to the CH₂ (a+b+c) of the ethylene units and the 1-butene units in the EB component but also to the CH₂ (d) of the main chain in the PS component.⁴⁸ The target is to separate the molecular motion of CH₂ groups of the ethylene units from the EB component upon heating. The temperature-dependent FTIR spectra cannot achieve this goal. Furthermore, no other characteristic means can be used to separate the molecular motion of CH₂ groups from the EB component.

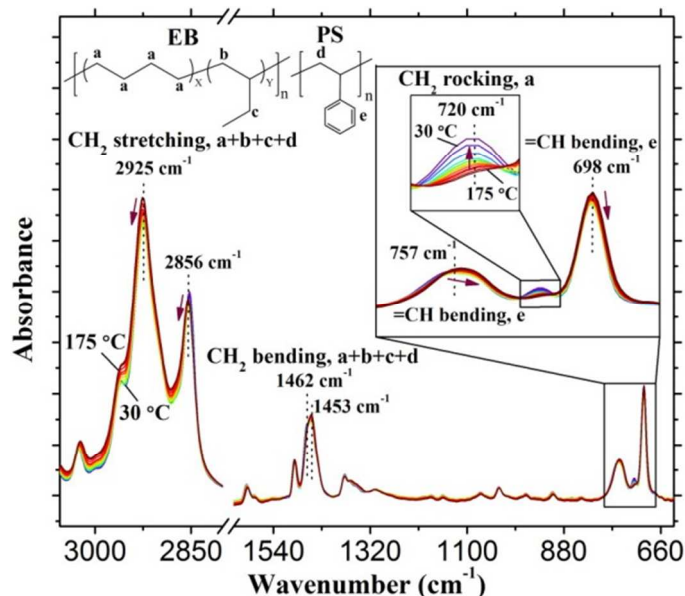


Figure 5. Temperature-dependent FTIR spectra of PS/EB in the 3055 cm^{-1} to 630 cm^{-1} region upon heating (30 °C to 175 °C). The bands at 2925 and 2856 cm^{-1} , which are serious overlapping bands, are assigned to the antisymmetric and symmetric stretching vibrations of CH₂. The bands at 720 cm^{-1} is the CH₂ rocking of the ethylene units of the EB component. The spectral intensity within the 730 cm^{-1} to 712 cm^{-1} region (720 cm^{-1} as the center) is selected as the projection matrix. The FTIR spectra within the 790 cm^{-1} to 670 cm^{-1} region are enlarged for clarity. For clear illustration, not all the collected FTIR spectra of PS/EB are shown.

4.2.2. Selection of the Projection Matrix

The projection matrix (or vector) must be determined to extract the molecular motion of CH₂ groups of the ethylene units. According to the literature,^{45, 48-52} the bands at 1462, 1453, and 720 cm^{-1} are attributed to CH₂ in the 1630 cm^{-1} to 630 cm^{-1} region. The bands at 1462 and 1453 cm^{-1} , which still show serious overlapping, are attributed to the CH₂ bending vibrations.⁴⁸⁻⁵¹ These two bands are actually the corresponding bending vibration of 2925 and 2856 cm^{-1} . Therefore, they cannot be used as the projection matrix (or vector). The bands at 720 cm^{-1} , which is the CH₂ rocking of the ethylene units of the EB component, is the characteristic bands of the ethylene units.^{45, 48, 52} This bands does not overlap with any bands of the PS component. The peak intensity of 720 cm^{-1} gradually weakened to disappear when the temperature increases from 30 °C to 175 °C. Thus, the intensity variation at 720 cm^{-1} indicates the microcrystalline melting of the ethylene units of the EB component. Therefore, 720 cm^{-1} is particularly

suitable for the projection matrix (or vector). With a somewhat different approach from PLLA/PBS, we select the spectral intensity within the 730 cm^{-1} to 712 cm^{-1} (720 cm^{-1} as the

center) region as the projection matrix rather than the projection vector.

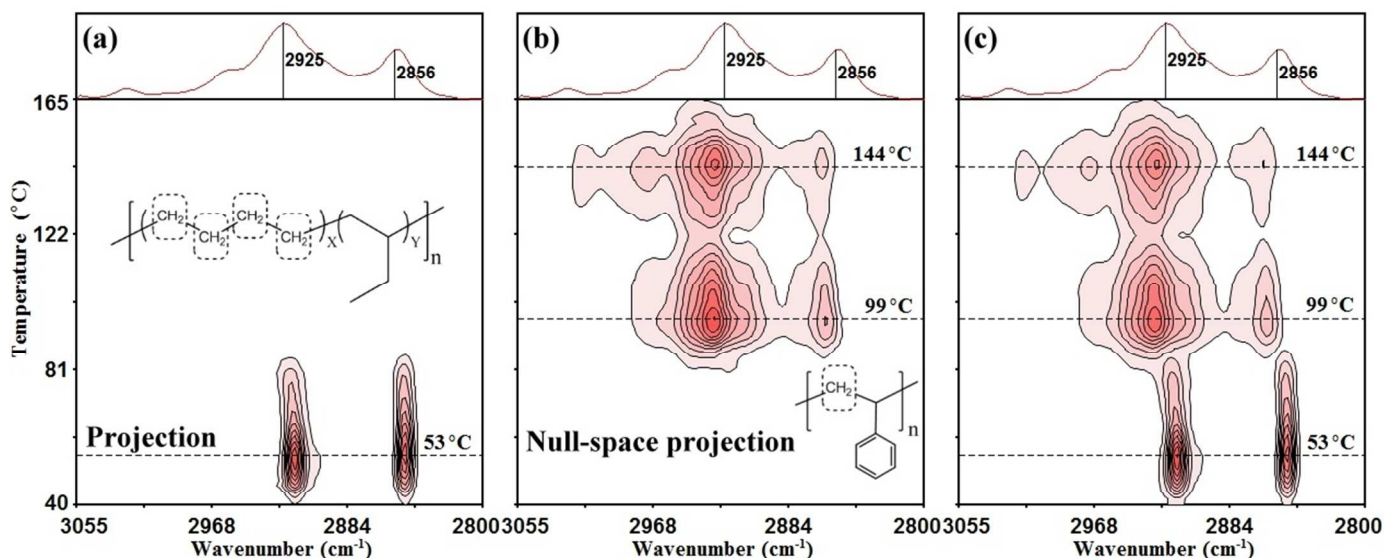


Figure 6. Key: (a) Proj-MW2D correlation FTIR spectrum of PS/EB ($40\text{ }^{\circ}\text{C}$ to $165\text{ }^{\circ}\text{C}$); (b) null-space Proj-MW2D correlation FTIR spectrum of PS/EB ($40\text{ }^{\circ}\text{C}$ to $165\text{ }^{\circ}\text{C}$); (c) conventional MW2D correlation FTIR spectrum ($40\text{ }^{\circ}\text{C}$ to $165\text{ }^{\circ}\text{C}$). The positive projection transformation algorithm is used for the calculations. The CH_2 motion during the microcrystalline melting of the ethylene units from the EB component is extracted into the Proj-MW2D correlation spectrum, and the temperature is $53\text{ }^{\circ}\text{C}$. The molecular motion of CH_2 groups of the main chain from the PS component is separated in the null-space Proj-MW2D correlation spectrum. However, the temperature is considerably high, namely, at $99\text{ }^{\circ}\text{C}$ and $144\text{ }^{\circ}\text{C}$, respectively.

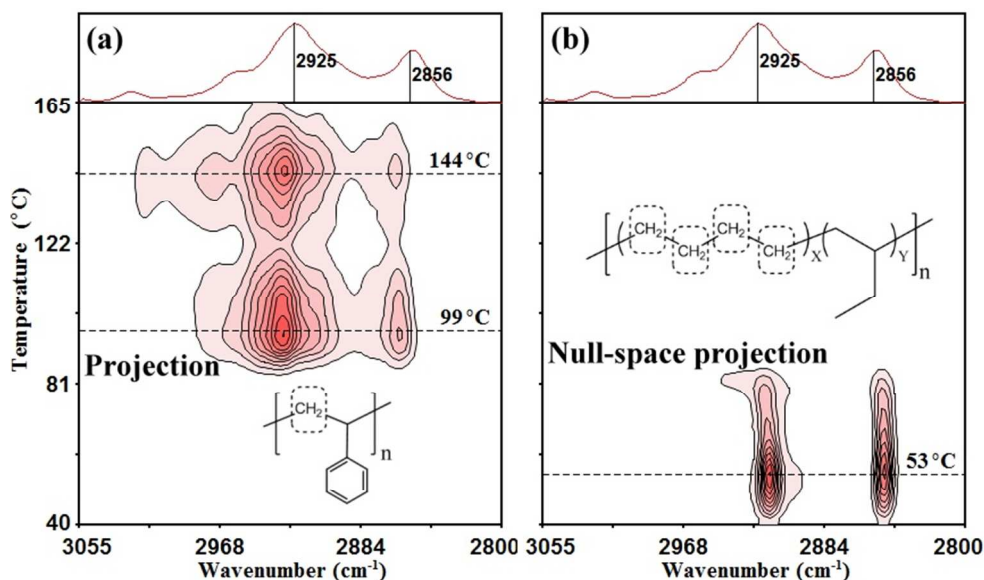


Figure 7. Key: (a) Proj-MW2D correlation FTIR spectrum of PS/EB ($40\text{ }^{\circ}\text{C}$ to $165\text{ }^{\circ}\text{C}$); (b) null-space Proj-MW2D correlation FTIR spectrum of PS/EB ($40\text{ }^{\circ}\text{C}$ to $165\text{ }^{\circ}\text{C}$). The positive projection transformation algorithm is used for the calculations. The spectral intensity within the 710 cm^{-1} to 687 cm^{-1} region (698 cm^{-1} as the center), which is assigned to the out-of-plane bending vibration of the $=\text{CH}$ of benzene rings of the PS component, is selected as the projection matrix. Once again, the molecular motion of CH_2 groups generated from the PS component is successfully extracted. The molecular motion of CH_2 groups of the ethylene units from the EB component is separated in the null-space Proj-MW2D correlation spectrum.

4.2.3. Proj-MW2D Analysis of the Molecular Motion of CH_2 Groups

The temperature-dependent FTIR spectra in the 3055 cm^{-1} to 2800 cm^{-1} were analyzed via the positive Proj-MW2D algorithm. **Figures 6(a)** and **6(b)** are the Proj-MW2D and

null-space Proj-MW2D correlation FTIR spectra of the PS/EB blend upon heating, respectively. The molecular motion of CH_2 groups with the same feature as the projection matrix 730 cm^{-1} to 712 cm^{-1} (720 cm^{-1} as the center) is retained in **Figure 6(a)**. The CH_2 motion in the ethylene units from the EB component is successfully separated. The correlation

intensity peaks appear at 2925 and 2856 cm^{-1} , and the temperature is 53 $^{\circ}\text{C}$, representing the CH_2 motion during the microcrystalline melting of the ethylene units from the EB component.^{17, 46}

In the null-space Proj-MW2D correlation spectra [Figure 6(b)], the CH_2 motion that is completely orthogonal (not identical) to the projection matrix is determined. That is, the molecular motion of CH_2 groups is not related to the ethylene units of the EB component [Figure 6(b)]. The correlation intensity peaks appear at 2925 and 2856 cm^{-1} but at high temperatures of 99 $^{\circ}\text{C}$ and 144 $^{\circ}\text{C}$, respectively. Two transition temperatures represent the molecular motion of CH_2 groups of the main chain from the PS component. According to the literature,⁵³⁻⁶² 99 $^{\circ}\text{C}$ is the glass transition temperature of PS.⁵³⁻⁵⁷ The temperature at 144 $^{\circ}\text{C}$ represents a liquid–liquid transition. Previous studies attributed this transition to the viscous flow of PS.⁵⁸⁻⁶²

Figure 6(c) shows the conventional MW2D correlation FTIR spectrum, which is a combination of the Proj-MW2D and null-space Proj-MW2D correlation spectra. The correlation intensity peaks appear at 2925 and 2856 cm^{-1} , and the corresponding temperatures are 53 $^{\circ}\text{C}$, 99 $^{\circ}\text{C}$, and 144 $^{\circ}\text{C}$. Although three transition temperatures can be observed, the conventional method cannot separate the molecular motion of CH_2 groups from EB or PS component without the help of other characterization methods. The conventional MW2D correlation FTIR spectra cannot indicate the source component of the transitions at the functional group level.

4.2.4. Separation of the Molecular Motion of CH_2 Groups from the Main Chain in PS

The above results suggest that the characteristic bands of the PS component can be employed as the projection matrix to extract the CH_2 motion of the main chain from PS component into the Proj-MW2D correlation FTIR spectrum. In Figure 5, the bands at 757 and 698 cm^{-1} are assigned to the out-of-plane bending vibration of the $=\text{CH}$ of benzene rings.⁵¹ In the present study, the spectral intensity within the 710 cm^{-1} to 687 cm^{-1} region (698 cm^{-1} as the center) is selected as the projection matrix. Within the entire temperature-dependent FTIR spectrum (Figure 5), the bands within 710 cm^{-1} to 687 cm^{-1} are characteristic of the PS component. The spectral intensities of these bands are relatively large and do not coincide with any of bands of the EB component. Therefore, 710 cm^{-1} to 687 cm^{-1} (698 cm^{-1} as the center) is a suitable projection matrix for extracting the CH_2 motion from PS component.

The Proj-MW2D and null-space Proj-MW2D correlation FTIR spectra are shown in Figures 7(a) and 7(b), respectively. The molecular motion with the same motion feature as the projection matrix (710 cm^{-1} to 687 cm^{-1}) is retained in Figure 7(a). Once again, the molecular motion of CH_2 groups from the PS component is successfully separated. These results confirm that the correlation intensity peaks of 2925 and 2856 cm^{-1} at 99 $^{\circ}\text{C}$ and 144 $^{\circ}\text{C}$ are the CH_2 motion of the main chain from the PS component. Figure 7(a) is

almost the same as Figure 6(b). Different from Figure 6, Figure 7(b) shows that the molecular motion of CH_2 groups of the ethylene units from the EB component is extracted in the null-space Proj-MW2D correlation FTIR spectrum. Similar to Figure 6(a), Figure 7(b) shows that the correlation intensity peaks of 2925 and 2856 cm^{-1} appear at 53 $^{\circ}\text{C}$. The use of 710 cm^{-1} to 687 cm^{-1} (698 cm^{-1} as the center) as the projection matrix can also separate the molecular motion of CH_2 groups generated from the PS component.

5. Conclusions

Proj-MW2D was developed to separate the molecular motion of groups generated from different components or phases for multicomponent and multiphase polymers. The specific implementation steps for Proj-MW2D were enumerated after the theoretical derivation and algorithm research.

Two types of two-component blends, namely, PLLA/PBS and PS/EB, were employed to validate the concept of separating the molecular motion of groups. The molecular motion of C=O groups from the crystalline phase in the PBS component was successfully extracted through the Proj-MW2D correlation FTIR spectra of PLLA/PBS upon cooling. The characteristic bands at 806 cm^{-1} of PBS was used as the projection vector. Meanwhile, the molecular motion of C=O groups from the PLLA component was separated in the null-space Proj-MW2D correlation FTIR spectrum. The PBS crystalline phase showed the C=O motion at 78 $^{\circ}\text{C}$. The molecular motion of C=O groups was generated from the PLLA component at 98 $^{\circ}\text{C}$.

The molecular motion of CH_2 groups during the microcrystalline melting of the ethylene units from the EB component was successfully extracted at 53 $^{\circ}\text{C}$ using the Proj-MW2D correlation FTIR spectra of PS/EB upon heating. The projection matrix was the spectral intensity of 730 cm^{-1} to 712 cm^{-1} (720 cm^{-1} as the center). The molecular motion of CH_2 groups of the main chain in the PS component was separated in the null-space Proj-MW2D correlation FTIR spectrum at 99 $^{\circ}\text{C}$ and 144 $^{\circ}\text{C}$.

This study successfully used the Proj-MW2D correlation technique to separate the molecular motion of groups for multiphase and multicomponent polymers. This method allows researchers to study the mechanism of the complex transition process for multiphase and multicomponent polymer systems.

In the future, Proj-MW2D can be extended to three- or four-component polymers, to other materials (e.g., small organic, biological, inorganic, and non-metallic materials), and to other spectra (e.g., Raman, X-ray, and UV). In addition, the projection technique was directly applied to MW2D correlation spectroscopy in this study. Nevertheless, it can be incorporated into PCMW2D methods and other forms of moving-window methods.

Acknowledgments

This work was supported by the National Natural Science Foundation of China (Grant Nos. 51473104, 51003066), State Key Laboratory of Polymer Materials Engineering (Grant No. sklpme2014-3-06), and the Outstanding Young Scholars Foundation of Sichuan University (Grant No. 2011SCU04A13).

Notes and references

^a State Key Laboratory of Polymer Materials and Engineering of China, Polymer Research Institute, Sichuan University, Chengdu 610065, China

* Corresponding author. Tel.: +86-28-85402601; Fax: +86-28-85402465; E-mail address: zhoutaopoly@scu.edu.cn.

1. T. R. Crompton, *Characterisation of Polymers*, Smithers Rapra Technology Limited, Shrewsbury, 2008.
2. T. Theophanides, *Infrared Spectroscopy-Materials Science, Engineering and Technology*, InTech, Rijeka, 2012.
3. B. Stuart, *Infrared Spectroscopy: Fundamentals and Applications*, John Wiley & Sons, 2004.
4. I. Noda, *Appl. Spectrosc.*, 1993, **47**, 1329-1336.
5. I. Noda and Y. Ozaki, *Two-dimensional Correlation Spectroscopy - Applications in Vibrational and Optical Spectroscopy*, John Wiley & Sons, Chichester, 2004.
6. I. Noda, *J. Mol. Struct.*, 2006, **799**, 2-15.
7. I. Noda, *J. Mol. Struct.*, 2008, **883-884**, 2-26.
8. I. Noda, *J. Mol. Struct.*, 2010, **974**, 3-24.
9. X. Liu, T. Zhou, X. Wang and J. Zhang, *Anal. Bioanal. Chem.*, 2010, **397**, 339-343.
10. H. Lee, Y. M. Jung, K. I. Lee, H. S. Kim and H. S. Park, *RSC Adv.*, 2013, **3**, 25944-25949.
11. Z. W. Wang and P. Y. Wu, *RSC Adv.*, 2012, **2**, 7099-7108.
12. M. Thomas and H. H. Richardson, *Vib. Spectrosc.*, 2000, **24**, 137-146.
13. S. Morita, H. Shinzawa, R. Tsenkova, I. Noda and Y. Ozaki, *J. Mol. Struct.*, 2006, **799**, 111-120.
14. H. H. Richardson and D. Wang, *J. Mol. Struct.*, 2010, **974**, 52-55.
15. S. Sasic, Y. Katsumoto, N. Sato and Y. Ozaki, *Anal. Chem.*, 2003, **75**, 4010-4018.
16. L. Hou and P. Y. Wu, *RSC Adv.*, 2014, **4**, 39231-39241.
17. T. Zhou, A. Zhang, C. S. Zhao, H. W. Liang, Z. Y. Wu and J. K. Xia, *Macromolecules*, 2007, **40**, 9009-9017.
18. T. Zhou, Z. Y. Wu, Y. Y. Li, J. A. Luo, Z. G. Chen, J. K. Xia, H. W. Liang and A. M. Zhang, *Polymer*, 2010, **51**, 4249-4258.
19. Y. Liu, W. L. Li, L. Hou and P. Y. Wu, *RSC Adv.*, 2014, **4**, 24263-24271.
20. S. Morita, H. Shinzawa, I. Noda and Y. Ozaki, *Appl. Spectrosc.*, 2006, **60**, 398-406.
21. J. A. Luo, T. Zhou, X. L. Fu, H. W. Liang and A. M. Zhang, *Eur. Polym. J.*, 2011, **47**, 230-237.
22. Z. Chen, T. Zhou, J. Hui, L. Li, Y. Li, A. Zhang and T. Yuan, *Vib. Spectrosc.*, 2012, **62**, 299-309.
23. Y. Li, T. Zhou, Z. Chen, J. Hui, L. Li and A. Zhang, *Polymer*, 2011, **52**, 2059-2069.
24. J. Shi, P. Wu and F. Yan, *Langmuir*, 2010, **26**, 11427-11434.
25. S. Sun, W. Zhang, W. Zhang, P. Wu and X. Zhu, *Soft Matter*, 2012, **8**, 3980-3987.
26. S. Sun and P. Wu, *Macromolecules*, 2013, **46**, 236-246.
27. I. Noda, *J. Mol. Struct.*, 2010, **974**, 116-126.
28. I. Noda, *J. Mol. Struct.*, 2010, **974**, 108-115.
29. H. Shinzawa, K. Awa, I. Noda and Y. Ozaki, *Vib. Spectrosc.*, 2013, **65**, 28-35.
30. M. K. Kim, S. R. Ryu, I. Noda and Y. M. Jung, *Vib. Spectrosc.*, 2012, **60**, 163-167.
31. G. H. Golub and C. F. Van Loan, *Matrix Computations* Johns Hopkins University Press, Baltimore, 1996.
32. L. Zheng, C. Li, D. Zhang, G. Guan, Y. Xiao and D. Wang, *Polym. Degradation Stab.*, 2010, **95**, 1743-1750.
33. H.-P. Zhao, J.-T. Zhu, Z.-Y. Fu, X.-Q. Feng, S. Yue and R.-T. Ma, *Thin Solid Films*, 2008, **516**, 5659-5663.
34. Y. J. Phua, N. S. Lau, K. Sudesh, W. S. Chow and Z. A. Mohd Ishak, *Polym. Degradation Stab.*, 2012, **97**, 1345-1354.
35. J. Zhang, K. Tashiro, H. Tsuji and A. J. Domb, *Macromolecules*, 2008, **41**, 1352-1357.
36. H.-S. Kim, H.-J. Kim, J.-W. Lee and I.-G. Choi, *Polym. Degradation Stab.*, 2006, **91**, 1117-1127.
37. H. S. Lee, H. D. Park and C. K. Cho, *J. Appl. Polym. Sci.*, 2000, **77**, 699-709.
38. C. Yan, Y. Zhang, Y. Hu, Y. Ozaki, D. Shen, Z. Gan, S. Yan and I. Takahashi, *The Journal of Physical Chemistry B*, 2008, **112**, 3311-3314.
39. J. Zhang, C. Li, Y. Duan, A. J. Domb and Y. Ozaki, *Vib. Spectrosc.*, 2010, **53**, 307-310.
40. P. Opaprakasit, M. Opaprakasit and P. Tangboriboonrat, *Appl. Spectrosc.*, 2007, **61**, 1352-1358.
41. E. Meaurio, E. Zuza, N. López-Rodríguez and J. R. Sarasua, *The Journal of Physical Chemistry B*, 2006, **110**, 5790-5800.
42. Y. Cai, J. Lv and J. Feng, *J. Polym. Environ.*, 2013, **21**, 108-114.
43. V. Krikorian and D. J. Pochan, *Macromolecules*, 2005, **38**, 6520-6527.
44. J. Zhang, Y. Duan, H. Sato, H. Tsuji, I. Noda, S. Yan and Y. Ozaki, *Macromolecules*, 2005, **38**, 8012-8021.
45. J. C. Sworen, J. A. Smith, J. M. Berg and K. B. Wagener, *J. Am. Chem. Soc.*, 2004, **126**, 11238-11246.
46. K. Jokela, A. Väänänen, M. Torckeli, P. Starck, R. Serimaa, B. Löfgren and J. Seppälä, *J. Polym. Sci., Part B: Polym. Phys.*, 2001, **39**, 1860-1875.
47. B. Crist and E. S. Claudio, *Macromolecules*, 1999, **32**, 8945-8951.
48. S. Krimm, *Advances in Polymer Science*, 1960, **2**, 51-172.
49. K. Holland-Moritz and E. Sausen, *Journal of Polymer Science: Polymer Physics Edition*, 1979, **17**, 1-23.
50. T. Ishioka, H. Wakisaka, I. Kanesaka, M. Nishimura and H. Fukasawa, *Polymer*, 1997, **38**, 2421-2430.
51. P. Sharma, P. Tandon and V. D. Gupta, *Eur. Polym. J.*, 2000, **36**, 2629-2638.
52. Y. Naka, N. Nemoto and Y. Song, *J. Polym. Sci., Part B: Polym. Phys.*, 2005, **43**, 1520-1531.
53. R. J. Roe and J. J. Curro, *Macromolecules*, 1983, **16**, 428-434.
54. B. Vorselaars, A. V. Lyulin and M. A. J. Michels, *Macromolecules*, 2007, **40**, 6001-6011.

55. J. D. Menczel and R. B. Prime, *Thermal Analysis of Polymers, Fundamentals and Applications*, John Wiley & Sons, Hoboken, 2009.
56. T. Hatakeyama and Z. H. Liu, *Handbook of thermal analysis* John Wiley & Sons, Chichester, 1998.
57. P. Painter, M. Sobkowiak and Y. Park, *Macromolecules*, 2007, **40**, 1730-1737.
58. C. Y. Liu and H. Morawetz, *Macromolecules*, 1988, **21**, 515-518.
59. T. Kanaya, T. Kawaguchi and K. Kaji, *The Journal of Chemical Physics*, 1996, **104**, 3841-3850.
60. S. Shang, X. Wu and Z. Zhu, *Physica B: Condensed Matter*, 2007, **396**, 160-163.
61. S. Shuying, Z. Zhenguang, L. Zaijun and Z. Guangzhao, *J. Phys.: Condens. Matter*, 2007, **19**, 416107.
62. T. Zhou, L. Peng, Y. Liu, A. Zhang and Y. Huang, *J. Mol. Struct.*, 2014, **1059**, 8-14.

